Gluon saturation and the Froissart bound: a simple approach

[1]F. Carvalho, [2]F.O. Durães, [3]V.P. Gonçalves and [1]F.S. Navarra
[1]*Instituto de Física, Universidade de São Paulo*
C.P. 66318, 05315-97, São Paulo, SP, Brazil
[2]*Dep. de Física, Centro de Ciências e Humanidades,*
Universidade Presbiteriana Mackenzie,
C.P. 01302-907, São Paulo, SP,Brazil
[3]*Instituto de Física e Matemática,*
Universidade Federal de Pelotas, Caixa Postal 354,
CEP 96010-900, Pelotas, RS, Brazil

At very high energies we expect that the hadronic cross sections satisfy the Froissart bound, which is a well-established property of the strong interactions. In this energy regime we also expect the formation of the Color Glass Condensate, characterized by gluon saturation and a typical momentum scale: the saturation scale Q_s. In this paper we show that if a saturation window exists between the nonperturbative and perturbative regimes of Quantum Chromodynamics (QCD), the total cross sections satisfy the Froissart bound. Furthermore, we show that our approach allows us to describe the high energy experimental data on $pp/p\bar{p}$ total cross sections.

PACS numbers: 12.38.-t,12.38.Aw,12.38.Bx

I. INTRODUCTION

Understanding the behavior of high energy hadron reactions from a fundamental perspective within Quantum Chromodynamics (QCD) is an important goal of particle physics. Since it was observed that the total hadronic cross sections grow with the center of mass energy ($\sqrt{s}$), much theoretical effort has been devoted to explain this growth. In particular, a QCD based explanation for this rising behavior was proposed by Gaisser and Halzen [1]: the cross section would grow because partons would start to play a role in the hadronic reactions. At higher energies, lower values of the Bjorken x are accessible and the parton distributions (especially the gluon distribution) grow very rapidly leading to rising cross sections. The basic idea of this approach, called minijet model, is that the total cross section can be decomposed as follows (see Fig. 1 (a)):

$$\sigma_{tot} = \int_0^{p_0^2} dp_T^2 \frac{d\sigma}{dp_T^2} + \int_{p_0^2}^{s/4} dp_T^2 \frac{d\sigma}{dp_T^2} = \sigma_0 + \sigma_{pQCD} \quad (1)$$

where σ_0 characterizes the nonperturbative contribution, which is in general taken as energy-independent at high energies [2], and σ_{pQCD} is calculable in perturbative QCD with the use of an arbitrary cutoff at low transverse momenta p_0. Unfortunately, this approach implies a power-like energy behavior for the total cross section, violating the Froissart bound, which is a consequence of the unitarity of the S matrix and states that total cross sections cannot grow faster than $\ln^2 s$ as $s \to \infty$. This bound is a well-established property of the strong interactions and puts a strict limit on the rate of growth with energy of the total cross sections. Over the years several solutions have been proposed to cure the too fast growth found in the minijet model [1], most of them using the eikonal formalism [3].

In parallel with these developments the study of the high energy limit of the linear evolution equations (DGLAP and BFKL) [4] revealed that they should be modified and gluon recombination effects (consequence of the high density of gluons) should be included in the QCD evolution [5]. This expectation can be easily understood: while for large momentum transfer $k_\perp$, the BFKL equation predicts that the mechanism $g \to gg$ populates the transverse space with a large number of small size gluons per unit of rapidity (the transverse size of a gluon with momentum $k_\perp$ is proportional to $1/k_\perp$), for small $k_\perp$ the produced gluons overlap and fusion processes, $gg \to g$, are equally important. Currently, one believes that the small-x gluons in a hadron wave function should form a Color Glass Condensate (CGC) which is described by an infinite hierarchy of coupled evolution equations for the correlators of Wilson lines [6, 7]. This new state of matter is characterized by gluon saturation and by a typical momentum scale, the saturation scale Q_s, which grows with the energy and determines the critical line separating the linear and saturation regimes of the QCD dynamics. The saturation effects are small for $k_\perp^2 > Q_s^2$ and very strong for $k_\perp^2 < Q_s^2$. Experimentally, there are strong evidences of nonlinear (saturation) effects at DESY-HERA. In particular, the DESY ep HERA data in the small-x and low-Q^2 region can be successfully described in terms of saturation models [8, 9, 10, 11, 12, 13, 14], with the measured cross sections presenting the geometric scaling property [15], which is an intrinsic property of the CGC physics. Moreover, the CGC physics is able to describe quite well the dAu RHIC data (see, e.g. Ref. [16]). These results give strong support to the existence of a saturation regime in the QCD dynamics (for recent reviews see, e.g., Ref. [6]).

Some attempts to reconcile the QCD parton picture with the Froissart limit using saturation physics were

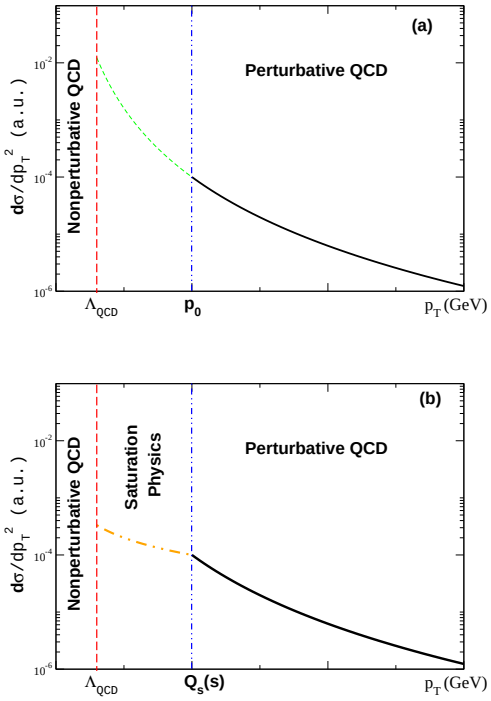

FIG. 1: Schematic behavior of the momentum distribution in the minijet model (a) and in the model proposed in this paper (b). While in the minijet model the region $\Lambda_{QCD} \leq p_T \leq p_0$ is disregarded, the region $\Lambda_{QCD} \leq p_T \leq Q_s(s)$ is included in our model and its contribution to the total cross section increases when the energy rises.

proposed in recent years, but the question remains open [17, 18, 19]. In this paper we propose a very simple phenomenological approach to treat this problem. In the next section we briefly describe the minijet model and how we include saturation effects in it. In the subsequent sections we present our numerical results and discuss them.

II. THE MINIJET MODEL WITH SATURATION

In what follows we generalize the minijet model assuming the existence of the saturation regime in the high energy limit. More precisely, we assume the existence of a saturation window between the nonperturbative and perturbative regimes of QCD, which grows when the energy increases (since Q_s grows with the energy). This window is shown in Fig. 1 (b). We now generalize Eq. (1) introducing the saturation window:

$$\sigma_{tot} = \int_0^{\Lambda^2_{QCD}} dp_T^2 \frac{d\sigma}{dp_T^2} + \int_{\Lambda^2_{QCD}}^{Q_s^2} dp_T^2 \frac{d\sigma}{dp_T^2} + \int_{Q_s^2}^{s/4} dp_T^2 \frac{d\sigma}{dp_T^2} = \sigma_0 + \sigma_{sat} + \sigma_{pQCD}\,, \quad (2)$$

where the saturated component, σ_{sat}, contains the dynamics of the interactions at scales lower than the saturation scale. In this region nonlinear effects are strong, changing the p_T behavior of the differential cross section, which becomes much less singular in the low p_T region, as we can see in Fig. 1 (b). The simple QCD collinear factorization formulas do not in general apply in this region.

A. σ_{pQCD}

At high transverse momenta we keep using the same collinear factorization formula employed in [1, 3] with the necessary update of the parton densities. The saturation scale arises as a natural cut-off at low transverse momenta of the perturbative (minijet) cross section component, σ_{pQCD}, which is now given by:

$$\sigma_{pQCD} = \frac{1}{2}\int_{Q_s^2} dp_T^2 \sum_{i,j} \int dx_1\, dx_2\, f_i(x_1, p_T^2)\, f_j(x_2, p_T^2)\, \hat{\sigma}_{ij} \quad (3)$$

where $f_i(x, Q^2)$ is the parton density of the species i in the proton extracted from deep inelastic scattering (DIS) and $\hat{\sigma}_{ij}$ is the leading order elementary parton-parton cross section. At very high energies the cross section (3) is dominated by gluon-gluon interactions. In what follows we use the MRST leading order parton distributions [20] in our calculations of σ_{pQCD}. Similar results are obtained using for instance the CTEQ6-LO parton distribution sets [21].

In order to evaluate σ_{pQCD} we need to specify Q_s, which is determined by the solution of the nonlinear evolution equation associated to CGC physics [6, 7]. It is given by:

$$Q_s^2(x) = Q_0^2 \left(\frac{x_0}{x}\right)^{\lambda} \quad (4)$$

where x is the Bjorken variable, with $Q_0^2 = 0.3$ GeV^2 and $x_0 = 0.3 \times 10^{-4}$ fixed by the initial condition. The saturation exponent λ has been estimated considering different approximations for the QCD dynamics, being ≈ 0.3 at NLO accuracy [22], in agreement with the HERA phenomenology, where the parameters Q_0, x_0 and λ were fixed by fitting the ep HERA data [8].

When we go from deep inelastic scattering to hadron - hadron collisions, there is some ambiguity in the definition of the equivalent of the Bjorken x. Following [23] we take x to be

$$x = \frac{q_0^2}{s} \quad (5)$$

where q_0 is a momentum scale to be determined. From (4) and (5) we immediately see that:

$$Q_s^2(s) \propto s^{\lambda} \quad (6)$$

with the constant of proportionality being determined by HERA data and our choice of q_0.

As it will be seen, in the high energy limit σ_{pQCD} is the most important contribution to σ_{tot}. With a constant infra-red cut-off, as in (1), it would grow too fast. The introduction of a cut-off increasing with energy can tame this growth, since the bulk of the integral in (3) comes from the low momentum region. This procedure was already employed, for example in [24], in a purely pragmatic approach. Here we establish a connection between this cut-off and the energy behavior of Q_s, controlled by the parameter λ in (6). Our procedure is more physical and, at the same time, imposes restrictions on λ.

B. σ_{sat}

In order to calculate the total cross section we also need to specify the saturated component. There are a few models for σ_{sat} [23, 25, 26]. Most of them are formulated in the color dipole picture, in which the projectile proton is treated as a color dipole, which interacts with the target proton. We shall use the model proposed in Ref. [23], in which the total cross section is given by:

$$\sigma_{sat} = \int d^2r |\Psi_p(r)|^2 \sigma_{dip}(x,r) \tag{7}$$

where r is the dipole transverse radius and the proton wave function Ψ_p is chosen to be:

$$|\Psi_p(r)|^2 = \frac{1}{2\pi S_p^2}\, exp\Big(-\frac{r^2}{2S_p^2}\Big) \tag{8}$$

with $S_p = 0.74$ fm and the dipole-proton cross section reads:

$$\sigma_{dip}(x,r) = 2\int d^2b \mathcal{N}(x,r,b) = \overline{\sigma}\mathcal{N}(x,r) \tag{9}$$

where $\overline{\sigma} = 2\pi R_p^2$, with $R_p = 0.9$ fm. The dipole scattering amplitude, $\mathcal{N}(x,r,b)$, should be given by the impact parameter dependent solution of a non-linear evolution equation, such as the Balitsky-Kovchegov equation [7]. A complete solution is not yet available and we would have to use models for $\mathcal{N}(x,r,b)$. In [23] it was assumed that $\mathcal{N}(x,r,b)$ falls exponentially with b. In this case σ_{sat} does not violate the Froissart bound. However in [18] it has been argued that the dipole amplitude decays only as a power of the impact parameter in the periphery of the proton and this dependence will, after integration in b, lead to logarithmic divergences. Here we prefer to avoid the use of models and, instead, assume the factorization implied by the second equality in (9). With this assumption we decouple the impact parameter and energy dependences and focus only on the energy behavior of the dipole and hadron-hadron cross sections.

In the literature there are many parameterizations of the dipole amplitude. A brief discussion of the features of some recent ones can be found in [16]. In what follows we shall use two of them, which were shown to give a reasonable description of both HERA and RHIC data [16]. Most of the parameterizations follow the Glauber-like formula originally introduced by Golec-Biernat and Wüsthoff [13]. The differences among them are in the anomalous dimension, γ. In the KKT model [9] the expression for the quark dipole-target forward scattering amplitude is given by [9]:

$$\mathcal{N}(r,x) \;=\; 1 - \exp\left[-\frac{1}{4}\left(r^2\,\bar{Q}_s^2\right)^{\gamma(Y,r^2)}\right]. \tag{10}$$

where $\bar{Q}_s^2 = \frac{C_F}{N_c}\,Q_s^2$ and the anomalous dimension $\gamma(Y,r^2)$ is

$$\gamma(Y,r^2) \;=\; \frac{1}{2}\left(1 + \frac{\xi(Y,r^2)}{\xi(Y,r^2) + \sqrt{2\,\xi(Y,r^2)} + 7\zeta(3)\,c}\right), \tag{11}$$

with c a free parameter (which was fixed in [9] to $c = 4$) and

$$\xi(Y,r^2) \;=\; \frac{\ln\left[1/(r^2\,Q_{s0}^2)\right]}{(\lambda/2)(Y - Y_0)}\,. \tag{12}$$

The authors of [9] assume that the saturation scale can be expressed by $Q_s^2(Y) = \Lambda^2 A^{1/3}\left(\frac{1}{x}\right)^{\lambda}$. The form of the anomalous dimension is inspired by the analytical solutions to the BFKL equation. Namely, in the limit $r \to 0$ with Y fixed we recover the anomalous dimension in the double logarithmic approximation $\gamma \approx 1 - \sqrt{1/(2\,\xi)}$. In another limit of large Y with r fixed, Eq. (11) reduces to the expression of the anomalous dimension near the saddle point in the leading logarithmic approximation $\gamma \approx \frac{1}{2} + \frac{\xi}{14\,c\,\zeta(3)}$. Therefore Eq. (11) mimics the onset of the geometric scaling region [11, 12]. In the calculations of Ref. [9] it is assumed that a characteristic value of r is $r \approx 1/(2\,k_T)$ where k_T is the transverse momentum of the valence quark and γ was approximated by $\gamma(Y,r^2) \approx \gamma(Y, 1/(4\,k_T^2))$. In the above expressions the parameters $\Lambda = 0.6$ GeV and $\lambda = 0.3$ are fixed by DIS data [13]. Moreover, the authors assume $Y_0 = 0.6$. The initial saturation scale used in (12) is defined by $Q_{s0}^2 = Q_s^2(Y_0)$ with Y_0 being the lowest value of rapidity at which the low-x quantum evolution effects are essential. As demonstrated in Ref. [9] this parameterization is able to describe the dAu RHIC data when the forward dipole cross section is convoluted with the respective fragmentation function and the parton distributions for the deuteron.

In Ref. [14] another phenomenological saturation model has been proposed in order to describe the dAu RHIC data (hereafter denoted DHJ model). The basic modification with respect to the KKT model is the parameterization of the anomalous dimension which is now given by

$$\gamma(Y,r^2) \;= \gamma_s + \Delta\gamma(Y,r^2) \tag{13}$$

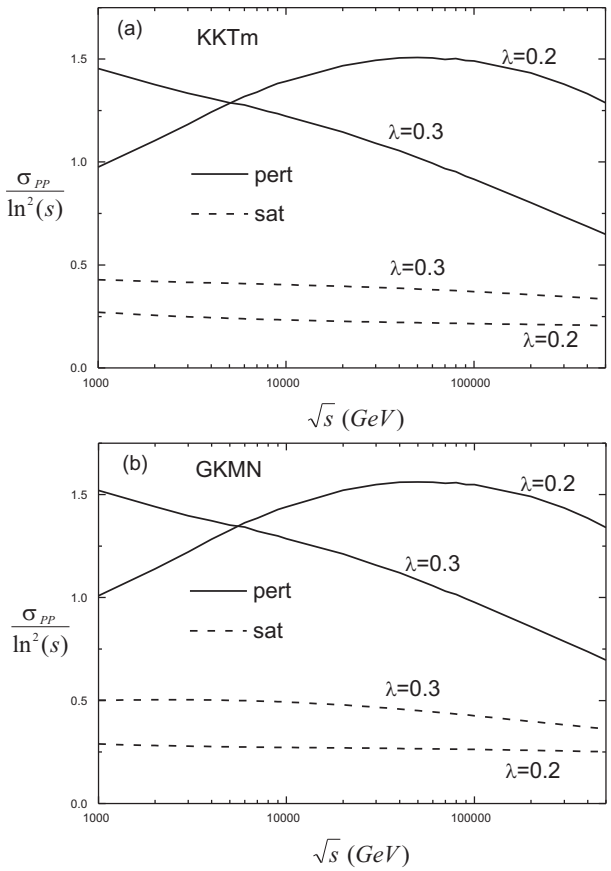

FIG. 2: Energy behavior of the perturbative (solid lines) and saturated components (dashed lines) of the total cross section (normalized by $\ln^2 s$ and in arbitrary units) for two different values of the exponent λ. In (a) and (b) we use the KKTm and GKMN dipole cross sections respectively. The perturbative component is the same.

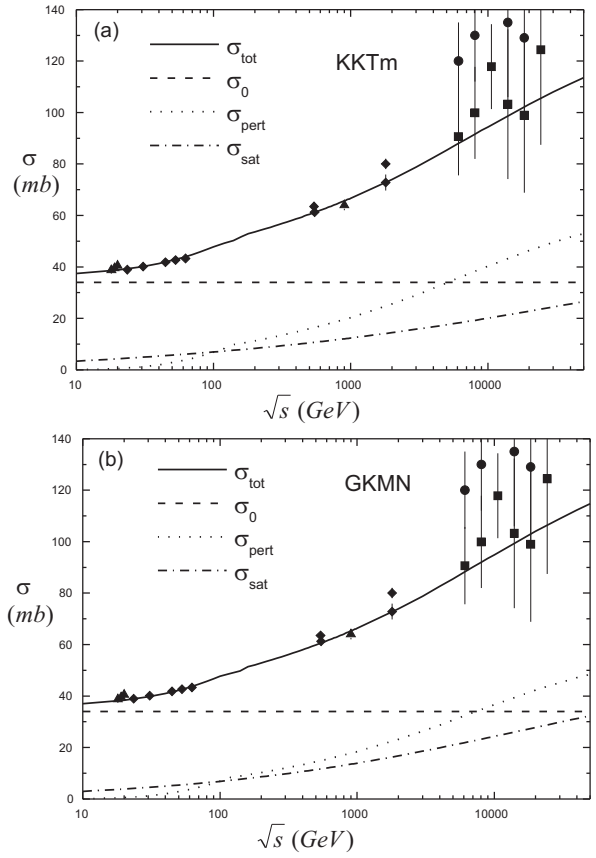

FIG. 3: Energy behavior of the total $pp/p\bar{p}$ cross section. The nonperturbative, perturbative and saturated components are presented separately as well as their sum, the total cross section. The results are for $\lambda = 0.25$. Data are from [28], [29], [30], [31] and from [32].

where

$$\Delta\gamma(Y, r^2) = (1-\gamma_s)\frac{|\log\frac{1}{r^2Q_T^2}|}{\lambda Y + |\log\frac{1}{r^2Q_T^2}| + d\sqrt{Y}} \ , \quad (14)$$

with $Q_T = Q_s(Y)$ a typical hard scale in the process, $\lambda = 0.3$ and $d = 1.2$. Moreover, $\gamma_s = 0.63$ is the anomalous dimension of the BFKL evolution with saturation boundary condition. Similarly to the KKT model this model is able to describe the dAu RHIC data.

As already discussed in Ref. [10], based on the universality of the hadronic wave function predicted by the CGC formalism, we might expect that the KKT and DHJ parameterizations would also describe the HERA data on proton structure functions in the kinematical region where the saturation effects should be present (small x and low Q^2). However, as shown in [16], this is not the case and neither KKT nor DHJ give an acceptable description of the HERA data on F_2.

Following Ref. [27] we consider a modification of the KKT model assuming that the saturation momentum scale is given by (4) , $Y_0 = 4.6$, $c = 0.2$ and that the typical scale in the computation of $\xi(Y, r^2)$ is the photon virtuality. This modified model will be called KKTm. We also use the modified version [16] of the DHJ model, called here GKMN, in which $Q_T = Q_0 = 1.0$ GeV, *i. e.* that the typical scale is energy independent.

In order to calculate σ_{sat}, it is also necessary to specify the Bjorken-x variable as in our previous calculations of σ_{pQCD}. We use the same prescription and the same value for q_0.

III. RESULTS

In Fig. 2 we show in arbitrary units the energy behavior of the ratios $\sigma_{pQCD}/\ln^2 s$ (solid lines) and $\sigma_{sat}/\ln^2 s$ (dotted lines) for two choices of λ. As it can be seen, all curves grow slower than $ln^2 s$. For smaller values of λ, such as λ (= 0.1) the fall of the ratio shown in Fig. 2 would be postponed to very high energies, $\sqrt{s} \simeq 10^6$ GeV. Although the energy at which the behavior of the cross section becomes "sub-Froissart" may depend

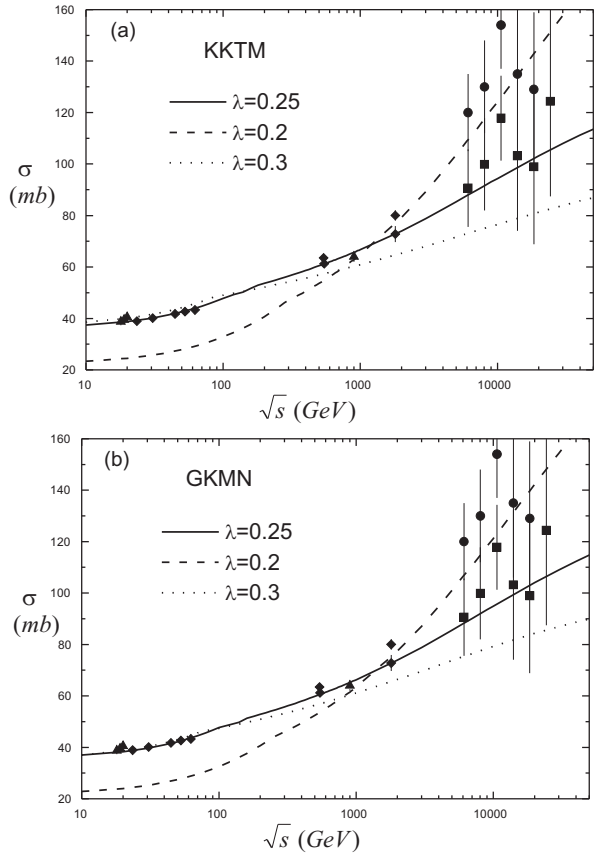

FIG. 4: Energy behavior of the total $pp/p\bar{p}$ cross section for different values of the exponent λ. Data are the same as in Fig. 3.

strongly on λ, one conclusion seems very robust: *once λ is finite, at some energy the growth of the cross section will become weaker than $ln^2 s$.*

After the study of the main properties of the perturbative and saturated components we can calculate the total cross section and compare with experimental data, obtained at CERN [28], at Fermilab Tevatron [29], [30] and in cosmic ray experiments [31, 32]. The latter refer to proton-air cross sections and were translated to proton-proton cross sections in the phenomenological study of Refs. [33, 34].

In Fig. 3 we show the sum $\sigma_0+\sigma_{sat}+\sigma_{pQCD}$ compared with the experimental data from Refs. [28, 29, 30, 31, 32]. σ_0 was taken to be 34 mb. In the figure the upper and lower panels were calculated with the KKTm and GKMN models, respectively. The values of q_0 were $q_0 = 0.044$ GeV and $q_0 = 0.038$ GeV respectively.

Considering that there is only one free parameter (q_0) in our approach, we obtain a good agreement with data. Moreover our predictions satisfy the Froissart bound. Probably a better agreement may be obtained if other quantities are treated as free parameters, as for instance the effective exponent λ, and included in a fitting procedure. As already mentioned, our results have a strong

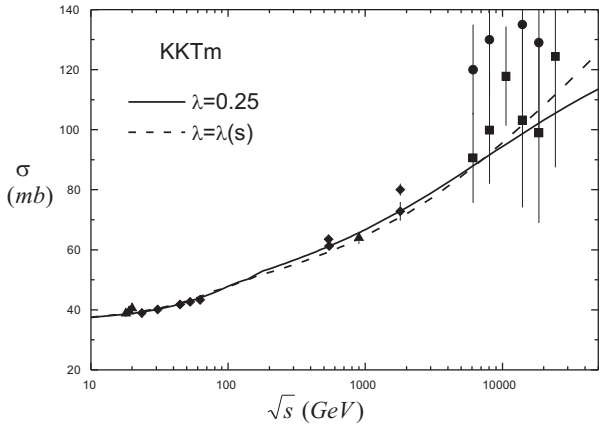

FIG. 5: Energy behavior of the total $pp/p\bar{p}$ cross section for different values of the exponent λ. Data are the same as in Fig. 3.

dependence on this quantity, as it can be seen in Fig. 4, where we present our results for the total cross section for different values of λ. It is important to emphasize that there is only a small range of values of λ which allow us to describe the experimental data. If, for instance, $\lambda = 0.4$ the resulting cross section is very flat and clearly below the data, while if $\lambda = 0.1$ the cross section grows very rapidly deviating strongly from the experimental data. The best choice for λ is in the range $0.25 - 0.3$, which is exactly the range predicted in theoretical estimates using CGC physics and usually obtained by the saturation models for the DESY *ep* HERA data.

In the theory of the CGC the parameter λ changes with the energy, being a function of the variable $Y = ln(1/x)$. Since our analysis is applied to a wide range of energies we have included the energy dependence of λ as estimated in [22], which can be parameterized as:

$$\lambda = 0.3 - 0.003(Y - 5) \tag{15}$$

In Fig. 5 we compare the cross sections obtained with a fixed value of λ (= 0.25) and obtained with a "running" λ, according to (15). As it can be seen, the difference between them is small.

IV. CONCLUSIONS

In this paper we have proposed a simple model for the total $pp/p\bar{p}$ cross section, which is an improvement of the minijet model with the inclusion of a window in the p_T-spectrum associated to the saturation physics. Our model implies a natural cutoff for the perturbative calculations which modifies the energy behavior of this component, so that it satisfies the Froissart bound. Moreover, including the saturated component (calculated with a dipole model), we obtain a satisfactory description of the experimental data. Our results for the total $pp/p\bar{p}$ cross section also satisfy the Froissart bound. Finally,

we find a very interesting consistency between our model and the saturation models used to describe the HERA data: similar values of λ are needed to describe both set of experimental data.

In other similar approaches, such as [23] the saturated cross section is used over the entire p_T domain, or equivalently, for dipoles of all sizes. This procedure has two disadvantages: it requires the introduction of an (model dependent) impact parameter dependence of the dipole cross section and it does not make use of the collinear factorization formula and the parton densities, which, in the high p_T region, are very well studied both theoretically and experimentally. In this sense our work is an improvement on [1] and on [23] as well.

Acknowledgements: This work was partially financed by the Brazilian funding agencies FAPESP, FAPERGS and CNPq.

[1] T. K. Gaisser and F. Halzen, Phys. Rev. Lett. **54**, 1754 (1985).

[2] See, for example, H. G. Dosch, E. Ferreira and A. Kramer, Phys. Rev. D **50**, 1992 (1994); H. G. Dosch, F. S. Navarra, M. Nielsen and M. Rueter, Phys. Lett. B **466**, 363 (1999).

[3] L. Durand and H. Pi, Phys. Rev. D **40**, 1436 (1989); Nucl. Phys. Proc. Suppl. **12**, 379 (1990); R. M. Godbole, A. Grau, G. Pancheri and Y. N. Srivastava, Phys. Rev. D **72**, 076001 (2005); E. G. S. Luna, A. F. Martini, M. J. Menon, A. Mihara and A. A. Natale, Phys. Rev. D **72**, 034019 (2005).

[4] For a review of these equations see, for example, V. Barone and E. Predazzi, "High Energy Particle Diffraction", Springer Verlag, Berlin, (2002).

[5] L. V. Gribov. E. M. Levin and M. G. Ryskin, Phys. Rep. **100**, 1 (1983).

[6] E. Iancu and R. Venugopalan, arXiv:hep-ph/0303204; A. M. Stasto, Acta Phys. Polon. B **35**, 3069 (2004); H. Weigert, Prog. Part. Nucl. Phys. **55**, 461 (2005); J. Jalilian-Marian and Y. V. Kovchegov, Prog. Part. Nucl. Phys. **56**, 104 (2006).

[7] I. Balitsky, Nucl. Phys. B **463**, 99 (1996); Y. V. Kovchegov, Phys. Rev. D **60**, 034008 (1999); Phys. Rev. D **61**, 074018 (2000).

[8] J. Bartels, K. Golec-Biernat and H. Kowalski, Phys. Rev **D66**, 014001 (2002); H. Kowalski and D. Teaney, Phys. Rev. D **68**, 114005 (2003).

[9] D. Kharzeev, Y.V. Kovchegov and K. Tuchin, Phys. Lett. **B599**, 23 (2004).

[10] M. S. Kugeratski, V. P. Gonçalves and F. S. Navarra, Eur. Phys. J. C **44**, 577 (2005).

[11] E. Iancu, K. Itakura, S. Munier, Phys. Lett. **B590**, 199 (2004).

[12] E. Iancu, K. Itakura and L. McLerran, Nucl. Phys **A708**, 327 (2002).

[13] K. Golec-Biernat and M. Wüsthoff, Phys. Rev. D **59** (1999) 014017, *ibid.* **D60**, 114023 (1999).

[14] A. Dumitru, A. Hayashigaki and J. Jalilian-Marian, Nucl. Phys. A **765**, 464 (2006); Nucl. Phys. A **770**, 57 (2006).

[15] A. M. Staśto, K. Golec-Biernat and J. Kwieciński, Phys. Rev. Lett. **86**, 596 (2001); V. P. Gonçalves and M. V. T. Machado, Phys. Rev. Lett. **91**, 202002 (2003); JHEP **0704**, 028 (2007); C. Marquet and L. Schoeffel, Phys. Lett. B **639**, 471 (2006).

[16] V. P. Gonçalves, M. S. Kugeratski, M. V. T. Machado and F. S. Navarra, Phys. Lett. B **643**, 273 (2006).

[17] E. Ferreiro, E. Iancu, K. Itakura and L. McLerran, Nucl. Phys. A **710**, 373 (2002).

[18] A. Kovner and U. A. Wiedemann, Phys. Rev. D **66**, 051502 (2002); Phys. Rev. D **66**, 034031 (2002); Phys. Lett. B **551**, 311 (2003).

[19] T. Ikeda and L. McLerran, Nucl. Phys. A **756**, 385 (2005).

[20] A. D. Martin, R. G. Roberts, W. J. Stirling and R. S. Thorne, Eur. Phys. J. C **23**, 73 (2002).

[21] J. Pumplin, D. R. Stump, J. Huston, H. L. Lai, P. Nadolsky and W. K. Tung, JHEP **0207**, 012 (2002).

[22] D. N. Triantafyllopoulos, Nucl. Phys. B **648**, 293 (2003).

[23] J. Bartels, E. Gotsman, E. Levin, M. Lublinsky and U. Maor, Phys. Lett. B **556**, 114 (2003).

[24] K. J. Eskola, K. Kajantie and K. Tuominen, Nucl. Phys. A **700**, 509 (2002); K. J. Eskola, P. V. Ruuskanen, S. S. Rasanen and K. Tuominen, Nucl. Phys. A **696**, 715 (2001).

[25] A. I. Shoshi, F. D. Steffen and H. J. Pirner, Nucl. Phys. A **709**, 131 (2002).

[26] B. Z. Kopeliovich, I. K. Potashnikova, B. Povh and E. Predazzi, Phys. Rev. Lett. **85**, 507 (2000); Phys. Rev. D **63**, 054001 (2001).

[27] M. V. T. Machado, Eur. Phys. J. C **47**, 365 (2006).

[28] A. S. Carrol et al., Phys. Lett. B61, 303 (1976); A. S. Carrol et al., Phys. Lett. B80, 423 (1979); U. Amaldi, and K. R. Schubert, Nucl. Phys. B166, 301 (1980); V. Bartenev et al., Phys. Rev. Lett. 31, 1089 (1973); N. A. Amos et al., Nucl. Phys. B262, 689 (1985); A. Breakstone et al., Nucl. Phys. B248, 253 (1984); M. Ambrosio et al., Phys. Lett. B115, 495 (1982); C. Augier et al., Phys. Lett. B316, 448 (1993).

[29] C. Augier et al., Phys. Lett. B **344**, 451 (1995); M. Bozzo et al., Phys. Lett. B **147**, 392 (1984); F. Abe et al., Phys. Rev. D **50**, 5550 (1994); N. A. Amos et al., Phys. Rev. Lett. **68**, 2433 (1992); C. Avila et al., Phys. Lett. B **537**, 41 (2002).

[30] C. Albajar et al., Nucl. Phys. B **309**, 405 (1988).

[31] Fly's Eye Collab., R.M. Baltrusaitis et al., Phys. Rev. Lett. **52**, 1380 (1984).

[32] AGASA Collab., M. Honda et al., Phys. Rev. Lett. **70**, 525 (1993).

[33] M.M. Block, F. Halzen and T. Stanev, Phys. Rev. D **62**, 077501 (2000).

[34] N. N. Nikolaev, Phys. Rev. D **48**, 1904 (1993).